Chinese Chemical Letters 36 (2025) 109762

Contents lists available at ScienceDirect

Chinese Chemical Letters

journal homepage: www.elsevier.com/locate/cclet

In situ formed fluorescent gold nanoclusters inhibit hair follicle regeneration in oxidative stress microenvironment *via* suppressing NFκB signal pathway

Xiangdong Lai, Tengfei Liu, Zengchao Guo, Yihan Wang, Jiang Xiao, Qingxiu Xia, Xiaohui Liu*, Hui Jiang*, Xuemei Wang*

State Key Laboratory of Digital Medical Engineering, School of Biological Science and Medical Engineering, Southeast University, Nanjing 210096, China

ARTICLE INFO

Article history:
Received 15 January 2024
Revised 8 March 2024
Accepted 11 March 2024
Available online 12 March 2024

Keywords:
Fluorescent gold nanoclusters
Skin injury
Reactive oxygen species
Hair follicle regeneration
Oxidative stress microenvironment

ABSTRACT

Skins expose to kinds of risk factors for damage, such as the hormone drugs, skin care products and ultraviolet radiation, which is accompanied by the production of excessive reactive oxygen species (ROS) and eventually leads to hypertrichosis. This skin disease is not aesthetically pleasing and even causes psychological and spiritual problems such as inferiority, anxiety and irritability. Current therapies are limited and often unsatisfactory, such as pharmacological and physical therapies, which have adverse effects and cause the irreversible destruction of hair follicles. Gold nanoclusters have good biocompatibility and their biosynthesis *in vivo* is responsive to oxidative stress microenvironment (OSM), which could be a safe and effective drug for ROS-induced skin injury. In our study, we demonstrated that zero valence fluorescent gold nanoclusters (FGNCs) were *in situ* biosynthesized in the plucking-induced damaged skin but not in the normal skin after the administration of gold precursors (+3), while FGNCs inhibited hair follicle regeneration by negatively regulating nuclear transcription factor kappa B (NFκB)-mediated inflammatory response signaling pathway (NFκB/tumor necrosis factor-α (TNF-α) axis). This OSM-responsive *in situ* biosynthesis method is facile and safe and holds great promise for curing hypertrichosis associated with skin dermatitis and injury.

The hair follicle is an essential accessory of the epidermis. Hair follicles not only produce hair but also are related to skin pigmentation [1–3]. Over the whole lifespan, the inferior segment of hair follicles undergoes periodic regression and reconstitution to control hair growth. Postnatal hair follicles renew cyclically in three phases: anagen, catagen, and telogen [4,5]. In the anagen stage, hair follicle stem cells (HFSCs) located in the niche of the bulge are activated with internal or external factors stimuli. Hair follicles grow down actively into the dermis until they reach their maximum length. Catagen is a transitional regression period from growth to quiescence. In the catagen stage, the lower cycling part of the hair follicle undergoes degradation and the dermal papilla is close to the bulge gradually. The telogen closely follows catagen. The proximity between the bulge and dermal papilla maintains in telogen. In this period, the hair follicles stop growing, and the dermal papilla becomes a naked small ball of cells. When hair growth activating signals come again, hair follicles reenter the anagen phase and begin to produce new hairs.

When the skin is damaged, the normal hair follicle cycle is disrupted. The long-term repeated administration of external hormone drugs and overuse of hormone-containing skin care products lead to hormone-dependent dermatitis, eventually appearing as hypertrichosis [6–10]. In addition, the skin injury is often accompanied by the production of large amounts of reactive oxygen species (ROS) [11–13], mediated by a respiratory burst in phagocytes and nicotinamide adenine dinucleotide phosphate (NADPH) oxidase in keratinocytes, fibroblasts and endothelial cells. Due to unpaired electrons, ROS are unstable and react easily with other molecules. Especially, excessive ROS cause oxidative damage to lipids and proteins on cell membranes and DNA in the nucleus and mitochondria [14,15]. Under oxidative stress, cells need to increase the yield of total antioxidants to maintain an equilibrium state [16,17]. Thus, there is an oxidative stress microenvironment (OSM) in the injured skin. Epidermal stem cells maintain the skin epithelium in healthy and oxidative stress conditions, and they are critical mediators of skin tissue adaptation to traumas [18]. Under

* Corresponding authors.
E-mail addresses: 101013182@seu.edu.cn (X. Liu), sungi@seu.edu.cn (H. Jiang), xuewang@seu.edu.cn (X. Wang).

https://doi.org/10.1016/j.cclet.2024.109762
1001-8417/

inflammatory distress, HFSCs stay in the activation state and drive hair follicle neogenesis after injury [19,20], resulting in hair regeneration.

Current therapies for hypertrichosis are not ideal. Pharmacotherapy, like eflornithine, shows severe side effects and unsatisfactory therapeutic effects [21–23]. Unwanted hair removal is painful and repetitive by physical therapies such as photo-epilation and electrolysis [24,25], which destroys hair follicles [26] and depletes cutaneous stem cell reservoirs, going against wound healing [27–32]. In the long run, these diseases will cause psychological distress to patients [22,33,34]. It is particularly important to develop a safer and more effective strategy than before. In recent years, studies have found that many *in vitro* synthesized metal and metal oxide nanoparticles have been used to protect skin cells from ROS, involving in gold nanoparticles, silver nanoparticles, iron oxide nanoparticles, cerium oxide nanoparticles, platinum nanoparticles and selenium nanoparticles [35–45]. Because of the relatively large diameter and the introduction of additional stabilizers and reductants in the process of synthesis, these *in vitro* synthesized nanoparticles cause toxicity to the organism. *In situ* biosynthetic FGNCs have good biocompatibility, and they are used for cancer imaging and treatment in many studies [46–55]. Especially, the bioinspired synthesized cytomembrane@AuNPs from intact MCF-7 cancer cells show the catalase-mimetic activity and act as a novel nano-antioxidant for cell protection from oxidative injury induced by ROS [56]. However, whether FGNCs can be synthesized in normal or injured skin cells is unknown. In this study, we took advantage of OSM in the damaged skin to synthesize FGNCs *in situ* through the hair plucking-induced injury model, while FGNCs inhibited the hair follicle regeneration by negatively regulating the nuclear transcription factor kappa B (NFκB) signal pathway. This facile and safe *in situ* biosynthesis method holds great promise for curing hypertrichosis associated with skin injury and dermatitis in future clinical applications.

Hair plucking causes a microinjury and an OSM, which activates HFSCs and leads to hair follicle regeneration [19,20,57–61]. Therefore, it is a good trauma model for investigating the response of $HAuCl_4$ precursors to the OSM and their effect on hair regeneration (Fig. S1 in Supporting information). C57BL/6 mice (20 ± 2 g) come from the Experimental Animal Center of Southeast University. The mice were allowed to eat and drink freely and fed under specific pathogen free (SPF)-grade conditions. All the animal experiments were permitted by the National Institute of Biological Science and Animal Care Research Advisory Committee of Southeast University. All the procedures involved in animal experiments were carried out per the guidelines of the Animal Research Ethics Board of Southeast University. Eight days after the first administration, the injection site in depilated mice injected $HAuCl_4$ precursors (DAu mice) showed the suppression of hair regeneration, whereas the skin of depilated mice injected phosphate buffer saline (PBS) (DPBS mice) turned black and the hair grew through camera photograph (Fig. 1a). The skin of hair-clipping mice injected $HAuCl_4$ precursors (HAu mice) showed no significant change, and the hair follicle cycle was still quiescence period. Furthermore, 12 days after hair plucking, hematoxylin-eosin (HE) staining of skin sections also demonstrated that the inhibition of hair follicle regeneration happened only in the injection site of DAu mice. All the hair follicles of DPBS mice entered anagen, and the hair follicles of HAu mice were still retained in the telogen phase (Fig. 1b).

In the OSM of the injured skin, whether $HAuCl_4$ precursors can be synthesized into gold nanoclusters is unknown. On account of specific fluorescence properties [62–66], gold nanoclusters were detected by fluorescence imaging system. And 3, 8, 24 h after the first intradermal injection, the mice were subjected to gas anesthesia with 2% isoflurane, and fluorescence images were captured through *in vivo* fluorescence imaging system under 480 nm excitation. The results revealed that the fluorescence signal of the dorsal skin among groups of mice showed no significant difference at 3 h. The injection site in DAu mice showed a strengthened fluorescence signal (up to 10^8 average radiant efficiency) at 8 and 24 h, respectively, compared to those in DPBS mice and HAu mice (Fig. S2 in Supporting information). It indicated that the FGNCs was synthesized only in the injured skin. Two days after the first drug administration, the main organs and drug-administrated skins were obtained for *ex vivo* fluorescent imaging. The results suggested that the fluorescence remained only in the dorsal skin injection site of DAu mice and there was no accumulation of FGNCs in the main organs (Fig. S3 in Supporting information).

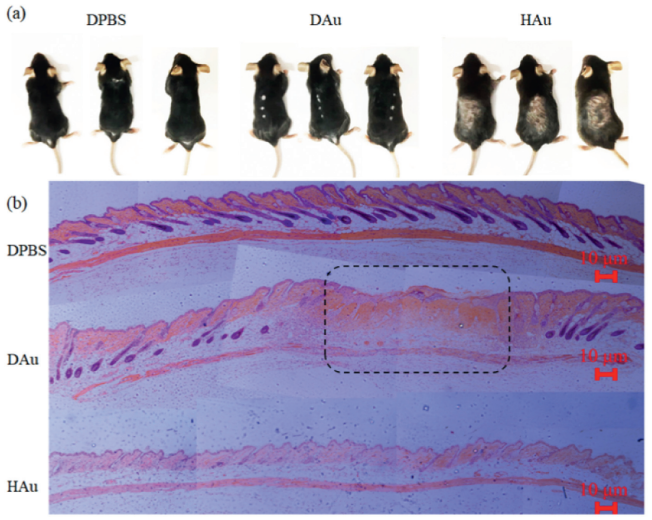

Fig. 1. (a) Camera photographs of DPBS, DAu, and HAu group of mice on the 9th day of the first administration. (b) HE staining of the paraffin-embedded skin tissue sections of different groups of mice. The dashed box indicates the site of administration and inhibition of the hair follicle regeneration. Each image comes from a combination of three or four photos taken in succession. Magnification: 100×.

To further confirm the biosynthesis of gold nanoclusters, we extracted them from the skin for the following characterization. Twelve hours after the first intradermal injection, FGNCs in the skin tissue at the injection site were extracted and characterized. As shown in (Figs. 2a and b), the typical transmission electron microscope (TEM) image and the diameter distribution curve demonstrated that most of *in situ* biosynthesized FGNCs ranged between 1.7 nm and 2.3 nm in diameter (with an average size of 1.99 nm). The particle size (below the clearance threshold ~5.5 nm) facilitated renal filtration and excretion, reducing the organ toxicity [67]. The morphology is predominantly spherical and the dispersion of the particles is very good without obvious aggregation at room temperature. From the observation of high-resolution TEM, the interplanar distance of FGNCs is 0.23 nm, which corresponds to the (111) planes of Au (the insert of Fig. 2b). Dark-field scanning transmission electron microscopy (STEM) and elemental mapping of FGNCs illustrated the distribution of Au, C, N, and O elements (Fig. S4 in Supporting information). Obviously, Au, N, C, and O elements were uniformly distributed, which revealed Au existing in skins. The maximum excitation and emission wavelengths were 462 and 525 nm from fluorescence spectra (Fig. 2c). X-ray photoelectron spectroscopy (XPS) was adopted to further demonstrate the valence state of gold (Fig. 2d). Four peaks were observed and coincided with the emission of 4f photoelectrons from Au(0) and Au(I). By calculating the integrated peak area, the atomic ratio of Au(0) and Au(I) co-existing in the samples was 83.7% and 16.3%, respectively. Energy dispersive spectrometer (EDS) showed that gold was present in the extract of skin tissue and the atomic percentage of gold was 0.29% (Fig. 2e and Table S1 in Supporting

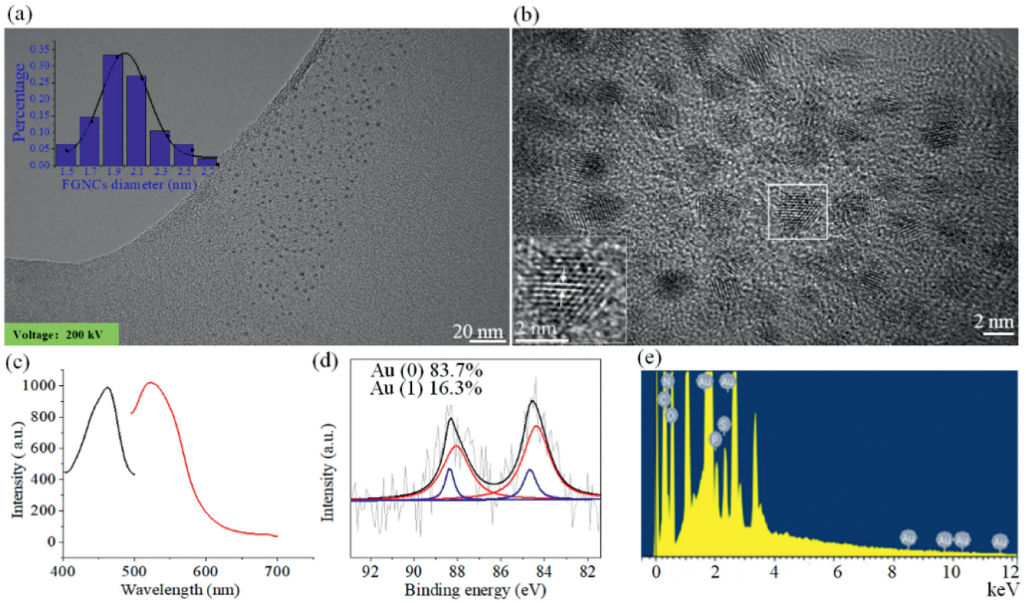

Fig. 2. Characterization of the extracted FGNCs. (a) TEM imaging of FGNCs. The insert of the blue histogram in the upper left corner showed the diameter distribution of FGNCs. (b) High resolution TEM imaging of FGNCs. (c) Fluorescence spectra of the FGNCs extracted from the skin showed that the maximum excitation and emission wavelengths were 462 and 525 nm, respectively. XPS and EDS analysis are respectively illustrated in (d) and (e).

information). The above results further confirmed that FGNCs were biosynthesized successfully.

Our previous results have revealed the particle size of FGNCs was suitable for clearance by renal filtration and there was no accumulation of FGNCs in the main organs. However, whether FGNCs cause tissue damage needs to be further evaluated. Twelve days after hair plucking, HE staining of the main organs showed that the *in situ* biosynthesized FGNCs caused no apparent toxicity (Fig. S5a in Supporting information). The body weight of DPBS, DAu, and HA mice was measured every three days. No significant changes in weights were found among the groups within 12 days after the first administration (Fig. S5b in Supporting information).

To further evaluate the biosafety of the *in situ* biosynthesized FGNCs, the blood was collected for hematology studies after the mice were euthanized. We carried out routine blood examinations and measured serum biochemical parameters. The results revealed no obvious difference in cell counting of erythrocytes, leukocytes, or platelets among groups of mice (Table S2 in Supporting information). In addition, the cardiac function index, namely creatine kinase (CK), liver function index, namely alanine transaminase (ALT) and aspartate transaminase (AST), and renal function index, namely urea and creatinine, demonstrated that the *in situ* biosynthesized FGNCs did not cause damage to the hearts, livers and kidneys of mice (Table S3 in Supporting information). In consequence, we concluded that the risk of severe side effects of FGNCs on normal organs and tissues was very low. This conclusion was consistent with that reported by Wang *et al.* who found that indeed spherical gold nanoparticles were not inherently toxic to HaCaT skin cells [68]. By and large, the *in situ* biosynthesized FGNCs are safe and promising for curing hypertrichosis associated with skin injury.

Though *in vivo* experiments have confirmed that biosynthesis of FGNCs occurs only in damaged skin, whether *in situ* biosynthesis is OMS-responsive needs to be further investigated. We scratched JB6 cells to simulate the damage of skin cells. After scratching the cells, ROS were only detected in the injured cells around the scratch by ROS assay kit (Fig. S6 in Supporting information). The undamaged cells in the negative control and scratch group showed no fluorescent DCF probes representing ROS production. The results suggested there was an OSM in the mechanically damaged skin cells. Subsequently, we confirmed that *in situ* biosynthesized FGNCs were present in this OSM. The medium with $HAuCl_4$ (pH 7) of different concentrations was incubated with JB6 cells for twenty-four hours. Cell viability was detected by CCK-8 assays. When the concentration of $HAuCl_4$ was up to 55 μmol/L, there was no obvious cytotoxicity (Fig. S7 in Supporting information). Therefore, we used 35 μmol/L $HAuCl_4$ solution in the following cell experiments. *In situ* synthesized FGNCs were only found in the injured cell around the scratch (Fig. S8 in Supporting information). Both the scratched cells without $HAuCl_4$ and the unscratched cells with $HAuCl_4$ showed no fluorescence signals. Some studies demonstrated $HAuCl_4$ can be taken into healthy human epithelial cells and Human embryonic kidney epithelial cells, and gold nanoparticles can be biosynthesized [69,70]. However, these studies showed the concentration dependence (1, 0.1 and 0.01 mmol/L) of the gold ionic reduction process is confirmed by negligible presence of gold nanoparticles in cells or cell culture supernatant, and the size of the synthesized gold nanoparticles (1–100 nm) is also concentration-dependent. Hence, we choose 35 μmol/L $HAuCl_4$ as the optimal concentration to treat JB6 and confirmed that the *in situ* biosynthesis of ultrasmall FGNCs is responsive to OSM. The transfer of $AuCl_4^-$ anions across the membrane is accomplished by diffusion [70]. The skin injury is often accompanied by ROS, resulting in stronger phospholipid peroxidation and higher destabilization and membrane permeability [71], which facilitates the uptake of $AuCl_4^-$. However, it is worth noting that the sequestration and reduction of $AuCl_4^-$ anions inside cells give rise to the progressive formation of gold nanoclusters, and this process will in turn have a positive effect on the uptake of $AuCl_4^-$ anions.

Hair plucking-induced injury causes an OSM and the inflammation response, activating HFSCs and leading to hair follicle regeneration [19,20,57,58]. OSM-responsive *in situ* biosynthesized FGNCs may inhibit hair follicle regeneration by suppressing inflammatory signaling pathway. Many changes in the biological phenotypes are often involved in gene expression, mainly reflected in the expression level and/or state of mRNA and protein. NFκB protein controls the expression of numerous downstream genes and regulates the pro-inflammatory and immune cellular responses, cell proliferation, and apoptosis [72–74]. The studies have reported that NFκB participates in the control of the mouse hair follicle

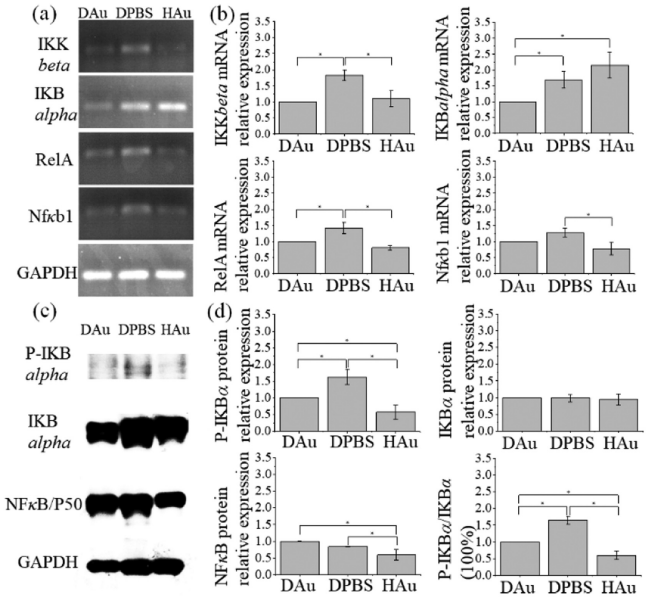

Fig. 3. The changes in expression of several key genes in the NFκB signalling pathway in the DAu, DPBS, and HAu groups, separately. RT-PCR results of four key molecules in the NFκB signalling pathway are presented in (a), and the corresponding semi-quantitative analysis of mRNA expression is presented in (b). Western blot results of the three main molecules in the NFκB signalling pathway are displayed in (c), and the corresponding semi-quantitative analysis of protein expression is presented in (d). Quantity One software was used to analyze the Western blot and RT-PCR results. The semi-quantitative analysis values in the DAu group were standardized to 1 and values for each group were expressed as mean ± standard deviation (SD) ($n = 3$). $^{*}P < 0.05$.

cycle, which is indispensable for HFSC activation, maintenance, and growth [75]. *In vitro* synthesized Au nanoparticles containing Diospyros kaki fruit extracts (DK-AuNPs) decreased ROS production, and the mitogen-activated protein kinases (MAPK)/NFκB signal pathway was involved in DK-AuNPs downregulating bioactive inflammatory markers in the skin [43]. AuNPs interact with cysteine (Cys-179) of inhibitor of kappa B kinase beta (IKKβ) and subsequently inhibit activation and nuclear translocation of NFκB [76]. Therefore, we have reasons to believe that the inhibition of the NFκB-mediated inflammatory response signal transduction is one of the main reasons why *in situ* biosynthesized FGNCs inhibit hair follicle regeneration. In the canonical NFκB signaling pathway, IKK phosphorylates inhibitor of kappa B (IKB), which makes IKB detach from the NFκB complex, and P50/P65 translocates into the cell nucleus, activating the transcription of inflammatory cytokines [77–83]. To further confirming that the *in situ* biosynthesized FGNCs can inhibit hair follicle regeneration by regulating the NFκB signal transduction, we investigated the expression of several critical molecules in the NFκB signaling pathway at mRNA and protein levels.

Eight days after the first drug administration, skins from DAu, DPBS, and HAu groups of mice were harvested, and total RNA was extracted for reverse transcription-polymerase chain reaction (RT-PCR). The results showed that the mRNA level of IKKβ and RelA in the skin of the DAu mice downregulated, compared to those in the skin of the DPBS group of mice (Figs. 3a and b). However, there were no significant differences in the level of mRNA expression of IKB alpha and Nfκb1 between the DAu and DPBS groups. Coinciding with mRNA expression, the expression of IKB alpha and NFκB/P50 protein level between the DAu and DPBS groups showed no significant differences (Figs. 3c and d). It was noteworthy that the level of phosphorylation-IKB (P-IKB) alpha and the proportion of P-IKB alpha/IKB alpha in DAu group decreased significantly, compared to these in DPBS group. The dephosphorylation of P-IKB prevented P50/P65 from translocating into the cell nucleus, resulting in the transcriptional inhibition of inflammatory factors. Tumor necrosis factor (TNF)-α is one of the NFκB-mediated proinflammatory cytokines [84]. We investigated the expression of TNF-α in the whole layer skin tissue at the different timepoints by enzyme-linked immunosorbent assay (ELISA). The results revealed the expression level of TNF-α in the DAu skin gradually decreased from 1 d to 4 and 8 d after hair plucking, and it remained unchanged in the DPBS skin (Fig. S9 in Supporting information). The results are consistent with Wang's and Chuong's reports that TNF-α activates HFSCs and hair regeneration after hair plucking-induced wound [19,20]. Hair follicles entered the growth phase immediately after plucking, and FGNCs in DAu skin negatively regulated NFκB/TNF-α, which inhibited hair regeneration. To observe the proliferation of hair follicle cells, skin tissues on the 9th day of the first administration were embedded in paraffin and sectioned. The expression of marker of proliferation Ki67 was observed by immunofluorescence staining (Fig. S10 in Supporting information). Compared with hair follicles in normal anagen in the DPBS skin and the non-administration site of the DAu skin (DAu-NA), the hair follicles in the administration site of the DAu skin (DAu-A) were smaller in size and were shorter in length. Hair matrix in DPBS and DAu-NA completely enveloped the dermal papilla, but it did not enclose or partially enclosed the dermal papilla in DAu-A. As indicated by the arrows, Ki67 was strongly expressed in hair matrix and outer root sheath in DPBS and DAu-NA, and it was weakly expressed in second hair germ and outer root sheath in DAu-A. The above results confirmed that *in situ* biosynthesized FGNCs inhibited hair follicle regeneration by negatively regulating NFκB-mediated inflammatory response signaling pathway.

Studies have proved that hair plucking causes microinjury and a cascade of inflammation, which activates HFSCs and leads to hair regeneration [19,20,57,58]. The increased total antioxidant status after hair plucking is an adaptive response to oxidative stress [60,61]. In the state of oxidative stress, cells must raise the level of antioxidants to maintain homeostasis [16,17], and increased antioxidants is conducive to the reduction of trivalent gold ions to low valence FGNCs. It has been reported that gold nanoclusters have the function of nano-enzymes that can scavenge ROS, thereby reducing the inflammatory damage caused by ROS [56,85–88]. The reason why FGNCs show the catalase mimetic activity is probably the presence of mixed valence gold atoms (0 and +1), reacting with hydrogen peroxide and superoxide to scavenge ROS. In addition, FGNCs can directly interact with cysteine (Cys-179) of IKKb and subsequently inhibit IKB/NFκB/TNF-α [76]. Our studies have confirmed that OSM-responsive biosynthetic FGNCs make both fluorescent imaging for the injured skin and inhibition of the hair follicle regeneration are readily realized. At first, we confirmed the production of ROS and fluorescent FGNCs only occured in scratch-injured cells. In addition, we similarly found that the FGNCs were biosynthesized only in hair-plucking injured skin and inhibited hair follicle regeneration by negatively regulating the NFκB-mediated inflammatory response signaling pathway (NFκB/TNF-α axis). The analyses of tissue section staining and hematology revealed the *in situ* biosynthesized FGNCs caused no apparent toxicity to the organism. Thus, the differential imaging diagnosis of the injured inflammatory skin and the normal skin can be realized, while the OMS-responsive *in situ* synthesized FGNCs are a safe and effective drug and hold great promise of therapeutic effect on hypertrichosis related to the skin inflammation and injury.

Declaration of competing interest

The authors declare that they have no known competing financial interests or personal relationships that could have appeared to influence the work reported in this paper.

Acknowledgments

This work was supported by the National Natural Science Foundation of China (Nos. 82061148012, 82027806, 82372220, 21974019), the National Key Research and Development Program of China (No. 2017YFA0205300), and the Primary Research & Development Plan of Jiangsu Province (No. BE2019716).

Supplementary materials

Supplementary material associated with this article can be found, in the online version, at doi:10.1016/j.cclet.2024.109762.

References

[1] M. Bejaoui, M.O. Villareal, H. Isoda, Front. Cell Dev. Biol. 8 (2020) 175.
[2] J. Lee, R. Bscke, P.C. Tang, et al., Cell Rep. 22 (2018) 242–254.
[3] M.R. Schneider, R. Schmidt-Ullrich, R. Paus, Curr. Biol. 19 (2009) R132–R142.
[4] W.J. Suen, S.T. Li, L.T. Yang, Stem Cells 38 (2020) 301–314.
[5] L. Alonso, E. Fuchs, J. Cell Sci. 119 (2006) 391–393.
[6] C. Erem, Acta Clin. Belg. 68 (2013) 268–274.
[7] D. Saleh, S.N.S. Yarrarapu, Hypertrichosis, 4th. ed., StatPearls, Florida, 2024.
[8] B.P. Messazos, M.R. Zacharin, J. Paediatr, Child Health 52 (2016) 1106–1110.
[9] K.F. Souza, P.F.B.C. Andrade, F.F. Cassia, M.C.R. Castro, An. Bras. Dermatol. 95 (2020) 402–403.
[10] D.S. Wendelin, D.N. Pope, S.B. Mallory, J. Am. Acad. Dermatol. 48 (2003) 161–182.
[11] C. Huang, L. Dong, B. Zhao, et al., Clin. Transl. Med. 12 (2022) e1094.
[12] Y. Zhu, K. Wang, X. Jia, et al., Med. Res. Rev. 44 (2024) 275–364.
[13] J.M. Jaffri, Malays. J. Med. Sci. 30 (2023) 7–20.
[14] J.G. Scandalios, Braz. J. Med. Biol. Res. 38 (2005) 995–1014.
[15] M. Pylvas, U. Puistola, L. Laatio, S. Kauppila, P. Karihtala, Anticancer Res. 31 (2011) 1411–1415.
[16] A.A. Franco, R.S. Odom, T.A. Rando, Free Radic. Biol. Med. 27 (1999) 1122–1132.
[17] B. Poljsak, Oxid. Med. Cell. Longev. 2011 (2011) 194586.
[18] S. Naik, S.B. Larsen, C.J. Cowley, E. Fuchs, Cell 175 (2018) 908–920.
[19] C.C. Chen, L. Wang, M.V. Plikus, et al., Cell 161 (2015) 277–290.
[20] X. Wang, H. Chen, R. Tian, et al., Nat. Commun. 8 (2017) 14091.
[21] R. Paparodis, A. Dunaif, Endocr. Pract. 17 (2011) 807–818.
[22] E.J. van Zuuren, Z. Fedorowicz, Br. J. Dermatol. 175 (2016) 45–61.
[23] N. Somani, D. Turvy, Am. J. Clin. Dermatol. 15 (2014) 247–266.
[24] E. Sharon, A. Levi, M. Lapidoth, I. Snast, Lasers Med. Sci. 38 (2023) 156.
[25] C.B. Barcaui, Dermatol. Surg. 33 (2007) 621–622.
[26] D. Lizneva, L. Gavrilova-Jordan, W. Walker, R. Azziz, Best Pract. Res. Clin. Obstet. Gynaecol. 37 (2016) 98–118.
[27] M.L. Martinez, E. Escario, E. Poblet, et al., J. Am. Acad. Dermatol. 75 (2016) 1007–1014.
[28] F. Heidari, A. Yari, H. Rasoolijazi, et al., Wounds 28 (2016) 132–141.
[29] J.D. Fox, K.L. Baquerizo-Nole, F. Van Driessche, et al., Wounds 28 (2016) 109–111.
[30] D.M. Ansell, J.E. Kloepper, H.A. Thomason, R. Paus, M.J. Hardman, J. Investig. Dermatol. 131 (2011) 518–528.
[31] C.L. Garcin, D.M. Ansell, Exp. Dermatol. 26 (2017) 101–104.
[32] F. Jimenez, E. Poblet, A. Izeta, Exp. Dermatol. 24 (2015) 91–94.
[33] A. Shrimal, S. Sardar, S. Roychoudhury, S. Sarkar, J. Cutan. Aesthet. Surg. 10 (2017) 40–44.
[34] W. Hafsi, J. Kaur, Hirsutism, 4th. ed., StatPearls, Florida, 2024.
[35] Y. Li, X. Hou, C. Yang, et al., Sci. Rep. 9 (2019) 2595.
[36] S. Chung, A.K. Roy, T.J. Webster, Int. J. Nanomed. 14 (2019) 9995–10007.
[37] K.E. Peloi, C.A. Contreras Lancheros, C.V. Nakamura, et al., Colloids Surf. B: Biointerfaces 191 (2020) 111013.
[38] F.M. Ribeiro, M.M. de Oliveira, S. Singh, et al., Front. Bioeng. Biotechnol. 8 (2020) 577557.
[39] E.S. Jun, Y.J. Kim, H.H. Kim, S.Y. Park, Mar. Drugs 18 (2020) 433.
[40] X. Zhai, C. Zhang, G. Zhao, et al., J. Nanobiotechnol. 15 (2017) 4.
[41] P.C. Wu, H.T. Hsiao, Y.C. Lin, D.B. Shieh, Y.C. Liu, Nanomedicine 13 (2017) 1975–1981.
[42] N. Tyagi, S.K. Srivastava, S. Arora, et al., Cancer Lett. 383 (2016) 53–61.
[43] S. Dhandapani, R. Wang, K. cheol Hwang, H. Kim, Y.J. Kim, Arab. J. Chem. 16 (2023) 104551.
[44] X. He, J. Xue, L. Shi, et al., Mater. Today Nano 17 (2022) 100149.
[45] Y. Xu, C. Li, J. An, et al., Sci. China Chem. 66 (2023) 155–163.
[46] C. Zhao, T. Du, F.u. Rehman, et al., Small 12 (2016) 6255–6265.
[47] J. Wang, G. Zhang, Q. Li, et al., Sci. Rep. 3 (2013) 1157.
[48] M. Wang, Y. Chen, W. Cai, et al., Proc. Natl. Acad. Sci. U. S. A. 117 (2020) 308–316.
[49] W. Cai, H. Feng, L. Yin, et al., eBioMedicine 54 (2020) 102740.
[50] W. Cai, L. Yin, H. Jiang, Y. Weizmann, X. Wang, Biosensors 11 (2021) 425.
[51] L. Yin, W. Cai, Y. Liang, et al., Aging 13 (2020) 241–261.
[52] Y. Wang, K. Huang, Z. Qin, et al., ACS Appl. Mater. Interfaces 14 (2022) 37291–37300.
[53] H. Xiong, J. Ye, M. Wang, et al., Biosens. Bioelectron. 218 (2022) 114763.
[54] F. Semcheddine, N. El Islem Guissi, W. Liu, et al., Mater. Horiz. 8 (2021) 2771–2784.
[55] W. Mi, S. Tang, S. Guo, H. Li, N. Shao, Chin. Chem. Lett. 33 (2022) 1331–1336.
[56] Y.S. Borghei, S. Hosseinkhani, Part. Part. Syst. Charact. 40 (2023) 2300006.
[57] D. Gay, O. Kwon, Z. Zhang, et al., Nat. Med. 19 (2013) 916–923.
[58] N. Ali, B. Zirak, R.S. Rodriguez, et al., Cell 169 (2017) 1119–1129. e11.
[59] A. Slominski, R. Paus, J. Investig. Dermatol. 101 (1993) 90S–97S.
[60] B. Kirschbaum, Clin. Chim. Acta 305 (2001) 167–173.
[61] R.L. Prior, G. Cao, Free Radic, Biol. Med. 27 (1999) 1173–1181.
[62] X. Ouyang, N. Jia, J. Luo, et al., JACS Au 3 (2023) 2566–2577.
[63] X. Zhou, X. Wang, L. Shang, Chin. Chem. Lett. 34 (2023) 108093.
[64] J. Sun, J. Li, X. Li, et al., Chin. Chem. Lett. 34 (2023) 107891.
[65] Y. Zhang, Y. Liu, Y. Yang, et al., Chin. Chem. Lett. 34 (2023) 108102.
[66] J. Qiao, X. Li, L. Qi, Chin. Chem. Lett. 33 (2022) 3193–3196.
[67] J. Wang, G. Liu, Angew. Chem. Int. Ed. 57 (2018) 3008–3010.
[68] S. Wang, W. Lu, O. Tovmachenko, et al., Chem. Phys. Lett. 463 (2008) 145–149.
[69] E. Larios-Rodriguez, C. Rangel-Ayon, S.J. Castillo, G. Zavala, R. Herrera-Urbina, Nanotechnology 22 (2011) 355601.
[70] Anshup, J.S. Venkataraman, C. Subramaniam, et al., Langmuir 21 (2005) 11562–11567.
[71] A. Gęgotek, K. Bielawska, M. Biernacki, I. Dobrzyńska, E. Skrzydlewska, Redox Biol. 12 (2017) 733–744.
[72] Y. Yamamoto, R.B. Gaynor, Curr. Mol. Med. 1 (2001) 287–296.
[73] R. Karki, O.J. Igwe, PLoS One 8 (2013) e73840.
[74] C. Gasparini, C. Celeghini, L. Monasta, G. Zauli, Cell. Mol. Life Sci. 71 (2014) 2083–2102.
[75] K. Krieger, S.E. Millar, N. Mikuda, et al., J. Investig. Dermatol. 138 (2018) 256–264.
[76] D. Zortéa, P.C. Silveira, P.S. Souza, et al., Ultrasound Med. Biol. 41 (2015) 151–162.
[77] A. Oeckinghaus, S. Ghosh, Cold Spring Harb. Perspect. Biol. 1 (2009) a000034.
[78] K. Taniguchi, M. Karin, Nat. Rev. Immunol. 18 (2018) 309–324.
[79] S. Prasad, V. Kumar, C. Singh, A. Singh, Inflammopharmacology 31 (2023) 1117–1147.
[80] W. Sun, Y. Gao, X. Yu, et al., Mol. Med. Rep. 18 (2018) 2733–2743.
[81] M.S. Hayden, S. Ghosh, Cell 132 (2008) 344–362.
[82] P. Viatour, M.P. Merville, V. Bours, A. Chariot, Trends Biochem. Sci. 30 (2005) 43–52.
[83] J. Zhang, J. Zhu, X. Chen, H. Xia, L. Yang, J. Dermatol. Sci. 107 (2022) 160–168.
[84] S. Kang, M. Amagai, Fitzpatrick's Dermatology, 9th ed., McGraw Hill Education, New York, 2019.
[85] J. Lou-Franco, B. Das, C. Elliott, C. Cao, Nano Micro Lett. 13 (2020) 10.
[86] Q. Dan, Z. Yuan, S. Zheng, et al., Pharmaceutics 14 (2022) 1645.
[87] R.A. Pinho, D.P.S. Haupenthal, P.E. Fauser, A. Thirupathi, P.C.L. Silveira, J. Inflamm. Res. 15 (2022) 3219–3234.
[88] A.P. Muller, G.K. Ferreira, A.J. Pires, et al., Mater. Sci. Eng. C: Mater. Biol. Appl. 77 (2017) 476–483.